



Contents lists available at ScienceDirect

ISA Transactions

journal homepage: www.elsevier.com/locate/isatrans

Practice article

Design of an adaptive super-twisting decoupled terminal sliding mode control scheme for a class of fourth-order systems

Donya Ashtiani Haghighi, Saleh Mobayen*

Electrical Engineering Department, University of Zanjan, Zanjan, Iran

ARTICLE INFO

Article history:

Received 7 October 2017

Received in revised form

14 January 2018

Accepted 5 February 2018

Available online xxx

Keywords:

Terminal sliding mode control

Decoupled sliding mode control

Adaptive tuning

Cart-pole system

Unknown uncertainties

ABSTRACT

This paper proposes an adaptive super-twisting decoupled terminal sliding mode control technique for a class of fourth-order systems. The adaptive-tuning law eliminates the requirement of the knowledge about the upper bounds of external perturbations. Using the proposed control procedure, the state variables of cart-pole system are converged to decoupled terminal sliding surfaces and their equilibrium points in the finite time. Moreover, via the super-twisting algorithm, the chattering phenomenon is avoided without affecting the control performance. The numerical results demonstrate the high stabilization accuracy and lower performance indices values of the suggested method over the other ones. The simulation results on the cart-pole system as well as experimental validations demonstrate that the proposed control technique exhibits a reasonable performance in comparison with the other methods.

© 2018 ISA. Published by Elsevier Ltd. All rights reserved.

1. Introduction

1.1. Background and motivation

In the past decades, the sliding mode control (SMC) technique has been extensively applied to the stabilization of various linear and nonlinear systems [1,2]. Its main advantages contain the robustness in contrast to parameter variations and external disturbances, guaranteed stability, fast response and easiness in employment. In general, the design process of SMC consists of two steps: (a) design of a suitable sliding surface; (b) design of a control law. The first step includes the selection of an appropriate switching surface such that makes the states of the system to stay along with it [3,4]. The second step concerns with the design of a suitable controller, which forces states of the system to reach the sliding surface [5,6]. When states of the system reach the sliding surface, the order of the control system is reduced and then, the system can dominate the certain external disturbances and matched uncertainties [7,8]. Nevertheless, the conventional SMC has some important weaknesses that the robustness of the control system is not satisfied in the reaching phase and there exists high-

frequency oscillations (chattering) in the control signal which is undesirable [9].

In order to realize finite-time convergence of the states, a new scheme of SMC method called terminal sliding mode control (TSMC) has been developed [10]. TSMC proposes some superior features such as high tracking accuracy, fast and finite-time convergence [11–13]. Although TSMC has been extensively employed to design the controller for linear and nonlinear systems [14,15], it TSMC suffers from the singularity phenomenon which produces an unbounded control input owing to the negative fractional power existed in the nonlinear sliding surface [16,17]. In TSMC, a nonlinear term is added to the sliding surface to improve the system's convergence [18,19]. This technique has not only the advantages of SMC, but also increases the stability performance of the system and speeds up the convergence rate near the equilibrium point [20,21]. In the recent years, a decoupled sliding mode control (DSMC) method has been planned which provides a simple procedure to decouple a class of fourth-order nonlinear systems into two second-order subsystems such that each subsystem contains a separate control purpose stated in terms of a switching surface [22,23]. A significant value of using DSMC is that the second subsystem is incorporated into the first subsystem by using a two-level decoupling scheme [24–26].

In the past decades, the super-twisting algorithm (STA) has been proposed as an alternative to conventional SMC technique [27–29]. STA scheme is extensively employed in various researches to

* Corresponding author. P.O. Box 38791-45371, Zanjan, Iran.

E-mail address: mobayen@znu.ac.ir (S. Mobayen).URL: http://www.znu.ac.ir/members/mobayen_saleh

decrease the chattering problem; because it does not require to measure the higher-order time-derivatives of the sliding surfaces [30,31]. STA is one of the most powerful second-order SMC algorithms introduced by Levant [32] which can handle a relative degree equal to one [33]. In general, STA creates a continuous control function which steers the sliding variable and its time-derivative to zero in the finite time in the existence of the smooth uncertainties with bounded gradient [34,35]. The algorithm guarantees robustness with regard to external disturbances and modeling errors while reducing the chattering problem originated in the conventional SMC [36]. Furthermore, STA obtains superior rapidity and stability to high-order SMC laws and prevents from acquiring the high-order derivative. STA has been effectively employed for several purposes such as state-estimation [37], tracking [38], synchronization [39], observation [40] and exact differentiation [41].

1.2. Literature review

In Ref. [42], a decoupled adaptive neuro-fuzzy DSMC scheme is proposed for the chaos control problem in a system without precise model information. However, the neuro-fuzzy DSMC control method of [42] is only applied for a Lorenz chaotic problem. A decoupled state-feedback and SMC technique is planned in Ref. [43] for three-phase PWM rectifier. Though, the proposed scheme of [43] is only employed for a three-phase PWM rectifier. Online optimal DSMC based on moving least squares and particle swarm optimization (PSO) procedures have been studied in Ref. [25]. But, the studied procedure in Ref. [25] has no analytical proofs for the stability of the controlled system. In Ref. [44], an adaptive robust PID control subject to supervisory DSMC based on genetic algorithm (GA) optimization approach is introduced. Nevertheless, reference [44] is based on a heuristic numerical algorithm. In Ref. [45], a DSMC technique is designed for a class of robots constituted by a chain of continuum segments named continuum arm. However, the dynamic equations of [45] are represented by a set of ordinary differential equations (ODE's) in time instead of partial differential equations (PDE's) in time and space. In Ref. [46], a disturbance estimator-based full-order DSMC method for a class of uncertain nonlinear multiple-input multiple-output (MIMO) systems is proposed. Though, the linear sliding surfaces have been used in the mentioned method of [46]. In Ref. [47], an adaptive neuro-interval type-2 fuzzy DSMC technique is applied on a three-dimensional crane system. Nevertheless, the parametric uncertainties are not considered in the three-dimensional crane model of [47]. Reference [22] suggests a nonsingular decoupled terminal sliding mode control (DTSMC) strategy for a class of fourth-order nonlinear systems. In Ref. [23], a time-varying sliding-coefficient-based DTSMC technique is presented for the fourth-order systems to make both subsystems converge to their equilibria in the finite time. In Ref. [48], a nonsingular DTSMC method is offered to address the tracking control problem of affine nonlinear systems. However, the adaptive approach has not employed in Refs. [22,23,48] for the estimation of the bound of external disturbances. A nonsingular DTSMC approach is planned in Ref. [26] for a three-degrees-of-freedom (3-DOF) parallel manipulator with actuation redundancy. Though, a radial basis function neural network (RBFNN) is applied to compensate the cross-coupling force and gravity of the parallel manipulator to improve the control precision. In Ref. [49], a tensor product model transformation based DTSMC design scheme is proposed. But, the parametric uncertainties have not been considered in the model of [49]. To the best of our knowledge, none of the studies mentioned above have been motivated on design of the adaptive decoupled terminal sliding mode control (ADTSMC) and adaptive super-twisting decoupled terminal sliding mode control (ASTDTSMC) schemes.

Moreover, the authors believe that any research has not been investigated on the chattering-free adaptive decoupled terminal sliding mode control on fourth-order systems with nonlinearities, parametric uncertainties and external disturbances which eliminates the necessity of the information about upper bounds of perturbations.

1.3. Contribution

In this paper, an adaptive super-twisting decoupled terminal sliding mode control method is investigated for a class of perturbed fourth-order systems. The control scheme is designed based on the Lyapunov stability theory. Furthermore, an adaptive gain-tuning law is adapted in the proposed DTSMC scheme which estimates the unknown upper bounds of the parametric uncertainties and external disturbances. Using the super-twisting algorithm approach, the chattering problem can be removed without any effectiveness on the stabilization performance. The numerical simulation confirms high stabilization accuracy and lower values of performance indices for the proposed technique compared to the other methods. Lastly, the proposed method is employed on an experimental cart-pole system to confirm the success and efficiency of this scheme. The main innovations of this paper compared to the related investigations are listed as follows:

- An adaptive super-twisting decoupled terminal sliding mode control scheme is designed for the stabilization of fourth-order systems;
- A suitable adaptive parameter-tuning law is suggested to dominate the perturbations of the system without the information of their upper bounds;
- A novel control procedure is proposed to establish a chattering-free robust performance and finite time convergence for both subsystems;
- The proposed technique is verified by demonstrative simulation results and experimental assessments.

1.4. Paper organization

The paper is organized as follows: in Section 2, the formulation of the fourth-order (cart-pole) system is given. The novel ASTDTSMC technique is presented in Section 3 as well as the stability analysis of the uncertain fourth-order system. In Section 4, the numerical simulation and experimental results on cart-pole system are prepared. Lastly, Section 5 gives concluding remarks.

2. Problem formulation

The considered fourth-order (cart-pole) system is in the form of under-actuated dynamical systems. This class of systems has fewer actuators than the degrees of freedom to be controlled [50]. Under-actuated dynamical systems have significant applications such as under-water robots, overhead crane, free-flying spacecraft, robotic manipulators, hypersonic vehicles, etc [51,52]. The stabilizer and tracker design for such systems requires a wide investigation. In the recent decade, much attention has been considered for the stabilization and tracking control of under-actuated systems. Several control approaches such as H_∞ control, input-output linearization, neural networks, backstepping control, SMC and Lyapunov redesign have been proposed to design appropriate controllers for these systems [53,54]. The under-actuated systems have many advantages, which contain lightening the system, decreasing the actuators' number and reducing the construction cost [55,56].

Consider the dynamic model of a cart-pole (single-inverted pendulum) system as [57]:

$$\begin{aligned}\dot{x}_1(t) &= x_2(t) \\ \dot{x}_2(t) &= f_1(x, t) + b_1(x, t)u_1(t) + d_1(t) \\ \dot{x}_3(t) &= x_4(t) \\ \dot{x}_4(t) &= f_2(x, t) + b_2(x, t)u_2(t) + d_2(t)\end{aligned}\quad (1)$$

where x_1, x_2, x_3 and x_4 represent the states; $f_1(x, t), f_2(x, t), b_1(x, t)$ and $b_2(x, t)$ denote the nonlinear functions representing system dynamics; b_1 and b_2 are non-zero functions; $u_1(t)$ and $u_2(t)$ indicate the control inputs; $d_1(t)$ and $d_2(t)$ signify external disturbances. The terms $f_1(x, t)$ and $f_2(x, t)$ can be expressed as

$$\begin{aligned}f_1(x, t) &= f_{01}(x, t) + \Delta f_1(t) \\ f_2(x, t) &= f_{02}(x, t) + \Delta f_2(t)\end{aligned}\quad (2)$$

where $f_{01}(x, t)$ and $f_{02}(x, t)$ are the known parts of $f_1(x, t)$ and $f_2(x, t)$, and $\Delta f_1(t)$ and $\Delta f_2(t)$ are the unknown parts of $f_1(x, t)$ and $f_2(x, t)$. The dynamic equation of (1) can also be written as

$$\begin{aligned}\dot{x}_1(t) &= x_2(t) \\ \dot{x}_2(t) &= f_{01}(x, t) + b_1(x, t)u_1(t) + n_1(t) \\ \dot{x}_3(t) &= x_4(t) \\ \dot{x}_4(t) &= f_{02}(x, t) + b_2(x, t)u_2(t) + n_2(t)\end{aligned}\quad (3)$$

where $n_1(t) = \Delta f_1(t) + d_1(t)$ and $n_2(t) = \Delta f_2(t) + d_2(t)$ are the terms of parametric uncertainties and external disturbances.

Assumption 1. The system perturbations are assumed to be bounded as $n_1 \leq \beta_1$ and $n_2 \leq \beta_2$, where β_1 and β_2 are unknown positive constants.

3. Adaptive super-twisting decoupled TSMC

DSMC technique is a way of decoupling a class of fourth-order nonlinear systems into two second-order subsystems which each subsystem has a separate control objective based on sliding surfaces [23,57]. The main objective is to propose a control strategy which steers the states of both subsystems from initial conditions to the sliding surfaces $S_1 = 0$ and $S_2 = 0$ and then, move along the sliding surfaces to the origin.

The nonlinear sliding surfaces for system (3) can be defined as

$$S_1 = \lambda_1(x_1 - z)^{\gamma_1} + \dot{x}_1 \quad (4)$$

$$S_2 = \lambda_2 x_3^{\gamma_2} + \dot{x}_3 \quad (5)$$

with

$$z = \text{sat}\left(\frac{S_2}{\phi_z}\right)z_U, \quad (6)$$

where λ_1 and λ_2 are positive constant; ϕ_z is the boundary layer of S_2 used to smooth z ; γ_1 and γ_2 are the fraction of two odd integers with conditions $0 < \gamma_1 < 1$ and $0 < \gamma_2 < 1$, z_U is the upper bound of $|z|$ with the condition $0 < z_U < 1$, which implies that the maximum absolute value of x_1 is limited. The first subsystem involves knowledge from the second one. In phase plane, $S_1 = 0$ and $S_2 = 0$ signify the lines with the slopes equal to $-\lambda_1$ and $-\lambda_2$, respectively. The control input which stabilizes both subsystems simultaneously can be obtained by embedding S_2 into S_1 through z .

Remark 1. It is sufficient to consider S_1 in the achievement of the controller because of the fact that the state knowledge in S_2 is transferred into S_1 via z and only, it is required to analyze the stability of first subsystem.

Now, differentiating (4) with respect to time and substituting (1) into it, we have

$$\dot{S}_1(t) = \lambda_1 \gamma_1 (x_2 - \dot{z})(x_1 - z)^{\gamma_1 - 1} + f_{01}(x, t) + b_1(x, t)u(t) + n_1(t) \quad (7)$$

Equating (7) to zero, the equivalent control law can be determined as.

$$u_{eq}(t) = \frac{-1}{b_1(x, t)} \times \left(\lambda_1 \gamma_1 (x_2 - \dot{z})(x_1 - z)^{\gamma_1 - 1} + f_{01}(x, t) \right) \quad (8)$$

where it can be observed that the perturbation term is not taken into account in (8). It is obvious that with considering the system uncertainties and external disturbances, the performance of the equivalent control law cannot be fulfilled. Hence, to eliminate the effects of the unwanted perturbations, an auxiliary controller should be designed. Moreover, suppose that $\hat{\beta}_1$ is the estimation value of β_1 which is estimated by the following adaptation law:

$$\dot{\hat{\beta}}_1 = \kappa_1 \|S_1(t)\|, \quad (9)$$

where κ_1 is a positive constant. The auxiliary control law can be defined as

$$u_{aux} = \frac{-1}{b_1(x, t)} \times \left(\hat{\beta}_1 \text{sgn}(S_1(t)) + MS_1(t) \right) \quad (10)$$

where M is a positive constant. The first term of (10) is an adaptive control law to compensate the perturbations. The term $MS_1(t)$ can be used to improve the dynamic performance and stability of the system. In addition, this term removes the error as a result of the perturbation in estimation. By increasing the value of M , the variations of the state variable will be reduced; though, the overshoot of the responses may be increased. On the other hand, by decreasing the value of M , the control gain will become small and the oscillation of the responses will be increased. The overall control law can be found from $u(t) = u_{eq}(t) + u_{aux}(t)$ as

$$u = \frac{-1}{b_1(x, t)} \times \left\{ \left(\lambda_1 \gamma_1 (x_2 - \dot{z})(x_1 - z)^{\gamma_1 - 1} + f_{01}(x, t) \right) + \left(\hat{\beta}_1 \text{sgn}(S_1(t)) + MS_1(t) \right) \right\}. \quad (11)$$

Theorem 1. Assume that the nonlinear sliding surfaces are in the form of (4) and (5), and the perturbation is unknown (but bounded), i.e., $n_1 \leq \beta_1$, where β_1 is the unknown positive constant.

Assume that $\hat{\beta}_1$ is the estimation of β_1 which is estimated by the adaptation law (9). The states of system (3) are converged to the sliding surfaces $S_1 = 0$ and $S_2 = 0$ in the finite time by using the adaptive control law (11), and remained on them thereafter.

Proof: Substituting control law (11) into (7), one obtains

$$\dot{S}_1(t) = - \left(\left(\hat{\beta}_1 \right) \text{sgn}(S_1(t)) + MS_1(t) \right) + n_1(t) \quad (12)$$

Construct the positive-definite Lyapunov candidate functional as.

$$V(t) = \frac{1}{2} S_1^2(t) + \frac{1}{2} \gamma_1 \hat{\beta}_1^2 \quad (13)$$

where $\tilde{\beta}_1 = \hat{\beta}_1 - \beta_1$. Taking the time-derivative of this Lyapunov function and using (9) and (12), we have

$$\begin{aligned}\dot{V} &= S_1(t)\dot{S}_1(t) + \gamma_1\tilde{\beta}_1\dot{\tilde{\beta}}_1 \\ &= n_1(t)S_1(t) - MS_1^2(t) - (\hat{\beta}_1)\|S_1(t)\| + \gamma_1(\hat{\beta}_1 - \beta_1)\kappa_1\|S_1(t)\| \\ &\leq \|n_1(t)\|\|S_1(t)\| - (\hat{\beta}_1)\|S_1(t)\| + \gamma_1(\hat{\beta}_1 - \beta_1)\kappa_1\|S_1(t)\| \\ &\quad + \beta_1\|S_1(t)\| - \beta_1\|S_1(t)\| \\ &\leq -(\beta_1 - \|n_1(t)\|)\|S_1(t)\| - (1 - \gamma_1\kappa_1)(\hat{\beta}_1 - \beta_1)\|S_1(t)\|\end{aligned}\quad (14)$$

By using $\|n_1\| \leq \beta_1$ and $\gamma_1\kappa_1 \leq 1$, hence, Eq. (14) can be obtained as (14)

$$\begin{aligned}\dot{V} &\leq -\sqrt{2}(\beta_1 - \|n_1(t)\|)\frac{|S_1(t)|}{\sqrt{2}} - \sqrt{\frac{2}{\gamma_1}}(1 - \gamma_1\kappa_1)\frac{\tilde{\beta}_1}{\sqrt{\frac{2}{\gamma_1}}}\|S_1(t)\| \\ &\leq -\min\left\{\sqrt{2}(\beta_1 - \|n_1(t)\|), \sqrt{\frac{2}{\gamma_1}}(1 - \gamma_1\kappa_1)\|S_1(t)\|\right\} \\ &\quad \times \left(\frac{|S_1(t)|}{\sqrt{2}} + \frac{\tilde{\beta}_1}{\sqrt{\frac{2}{\gamma_1}}}\right) = -\Omega V^{\frac{1}{2}}.\end{aligned}\quad (15)$$

where $\Omega = \min\left\{\sqrt{2}(\beta_1 - \|n_1(t)\|), \sqrt{\frac{2}{\gamma_1}}(1 - \gamma_1\kappa_1)\|S_1(t)\|\right\}$. In

conclusion, by using the adaptive-tuning control law (11), the finite time convergence to the switching surface $S_1(t) = 0$ is satisfied. The suggested control scheme forces the sliding surface S_1 to approach to $x_1 = z$ and $x_2 = 0$ in the finite time. The state x_2 converges to the origin if and only if z converges to zero, which indicates that S_2 approaches to zero. Therefore, it can be established that all state variables converge to the origin and the stabilization purpose of both subsystems are attained.

Remark 2. The adaptive control law (11) can be modified by a saturation function instead of the sign function to avoid the chattering problem. However, a wide boundary layer may cause the steady-state error and a narrow boundary layer cannot remove the chattering problem.

The super-twisting algorithm is a suitable alternative to the saturation function to avoid the chattering phenomenon without affecting the tracking performance. For this purpose, in the following theorem, the adaptive decoupled TSMC is combined with the super-twisting sliding-mode algorithm.

Theorem 2. Assume that the sliding surfaces are in the form of (4) and (5). If the adaptive super-twisting decoupled TSMC law is designed as

$$\begin{aligned}u &= \frac{-1}{b_1(x, t)} \times \left(\lambda_1 \gamma_1 \left(\dot{x}_1 - \dot{z} \right) (x_1 - z)^{\gamma_1 - 1} \right. \\ &\quad \left. + f_{01}(x, t) + L_1 |S_1|^{\frac{1}{2}} \text{sgn}(S_1) + \hat{\beta}_1 + w \right) \\ \dot{w} &= -L_2 \text{sgn}(S_1)\end{aligned}\quad (16)$$

with

$$\dot{\tilde{\beta}}_1 = \frac{-1}{|z_1|} H_1^T P Z \quad (17)$$

where $w \in \mathbb{R}$ is state of the super-twisting controller, and L_1 and L_2 are the constant positive gains, then, the state variables of both subsystems are stabilized.

Proof: Consider the positive-definite Lyapunov function as

$$V(\tilde{z}, \tilde{\beta}_1) = \tilde{z}^T P \tilde{z} + \frac{1}{2} \Gamma \tilde{\beta}_1^T \tilde{\beta}_1 \quad (18)$$

where Γ is a positive scalar, P is a positive-definite matrix, and $z = [z_1, z_2]^T$ is defined as

$$\begin{aligned}z_1 &= |S_1|^{1/2} \text{sgn}(S_1) \\ z_2 &= w\end{aligned}\quad (19)$$

It ensures from (19) that S_1 and w approach to the origin as z_1 and z_2 converge to zero. From (16) and (19), the time-derivative of Z can be obtained as

$$\dot{Z} = \begin{bmatrix} \frac{\partial z_1}{\partial S_1} \dot{S}_1 \\ \frac{\partial z_2}{\partial w} \dot{w} \end{bmatrix} = \begin{bmatrix} \frac{\dot{S}_1}{2|S_1|^{1/2}} \\ -L_2 \text{sgn}(S_1) \end{bmatrix} = \frac{1}{|z_1|} \begin{bmatrix} \frac{1}{2} \dot{S}_1 \\ -L_2 z_1 \end{bmatrix} \quad (20)$$

Now, substituting (7) and (16) into (20) and considering the upper bound of $n_1(t)$, one achieves

$$\dot{Z} = \frac{1}{|z_1|} \begin{bmatrix} \frac{1}{2} (-L_1 z_1 - z_2 - \tilde{\beta}_1) \\ -L_2 z_1 \end{bmatrix}. \quad (21)$$

Eq. (21) can be rewritten as

$$2|z_1|\dot{Z} = AZ + H_1\tilde{\beta}_1 \quad (22)$$

where $A = \begin{bmatrix} -L_1 & 1 \\ 2L_2 & 0 \end{bmatrix}$ and $H_1 = \begin{bmatrix} -1 \\ 0 \end{bmatrix}$.

Construct the Lyapunov candidate function as

$$V_0(Z) = Z^T P Z \quad (23)$$

where by differentiating the Lyapunov function (23) and using (22), one can obtain

$$\begin{aligned}2|z_1|\dot{V}_0(Z) &= 2|z_1|\dot{Z}^T P Z + 2Z^T P |z_1|\dot{Z} \\ &= Z^T (A^T P + P A) Z + (H_1 \tilde{\beta}_1)^T P Z + Z^T P (H_1 \tilde{\beta}_1)\end{aligned}\quad (24)$$

Hence, we require

$$A^T P + P A = -Q_0 < 0 \quad (25)$$

where Q_0 is a uniformly positive-definite matrix and there exists a constant positive-definite matrix P if and only if A is Hurwitz.

Now, using (24) and time-derivative of (18), we have

$$\begin{aligned}\dot{V}(\tilde{z}, \tilde{\beta}_1) &= \frac{1}{2|z_1|} \dot{V}_0(Z) + \frac{1}{|z_1|} Z^T P H_1 \tilde{\beta}_1 + \Gamma \tilde{\beta}_1^T \dot{\tilde{\beta}}_1 \\ &= -\frac{1}{2|z_1|} Z^T Q_0 Z + \frac{1}{|z_1|} Z^T P H_1 \tilde{\beta}_1 + \Gamma \tilde{\beta}_1^T \dot{\tilde{\beta}}_1\end{aligned}\quad (26)$$

Choosing the adaptation law as (17), then the term $\frac{1}{|z_1|} Z^T P H_1 + \Gamma \tilde{\beta}_1^T$ in (26) can be removed and one can obtain $\dot{V}(\tilde{z}, \tilde{\beta}_1) < 0$. Hence, by the suggested control scheme (16), one can conclude that the states are converged to zero and the stabilization purpose of both subsystems is achieved. Moreover, this super-twisting algorithm is a suitable function to remove the chattering phenomenon without affecting the stabilization performance.

In this section, we consider a special choice of the Lyapunov

function (18) which allows removing the singularity in the adaptation law. Let

$$P = \begin{bmatrix} 1 & 0 \\ 0 & P_2 \end{bmatrix}, \quad (27)$$

with $P_2 > 0$. Due to the structure of H_1 , the adaptation law (17) is simplified to

$$\hat{\beta}_1 = \frac{1}{T} \text{sgn}(S_1). \quad (28)$$

4. Simulation and experimental results

In order to validate the suggested control technique, a cart–pole system is simulated and some comparisons between the suggested technique and the methods of [23] and [57] are presented.

The dynamic behavior of the cart–pole system illustrated in Fig. 1 can be presented in the form of (3) with the functions $f_{01}(x, t)$, $b_1(x, t)$, $f_{02}(x, t)$ and $b_2(x, t)$ as

$$\begin{aligned} f_{01}(x, t) &= \frac{m_t g \sin(x_1) - m_p L \sin(x_1) \cos(x_1) x_2^2}{L \left(\left(\frac{4}{3} \right) m_t - m_p \cos^2(x_1) \right)} \\ b_1(x, t) &= \frac{\cos(x_1)}{L \left(\left(\frac{4}{3} \right) m_t - m_p \cos^2(x_1) \right)} \\ f_{02}(x, t) &= \frac{-\left(\frac{4}{3} \right) m_p L x_2^2 \sin(x_1) + m_p g \sin(x_1) \cos(x_1)}{\left(\frac{4}{3} \right) m_t - m_p \cos^2(x_1)} \\ b_2(x, t) &= \frac{4}{3 \left(\left(\frac{4}{3} \right) m_t - m_p \cos^2(x_1) \right)} \end{aligned} \quad (29)$$

where $x_1(t)$ represents the angular position of the pole from the vertical axis, $x_2(t)$ signifies the angular velocity of the pole from the

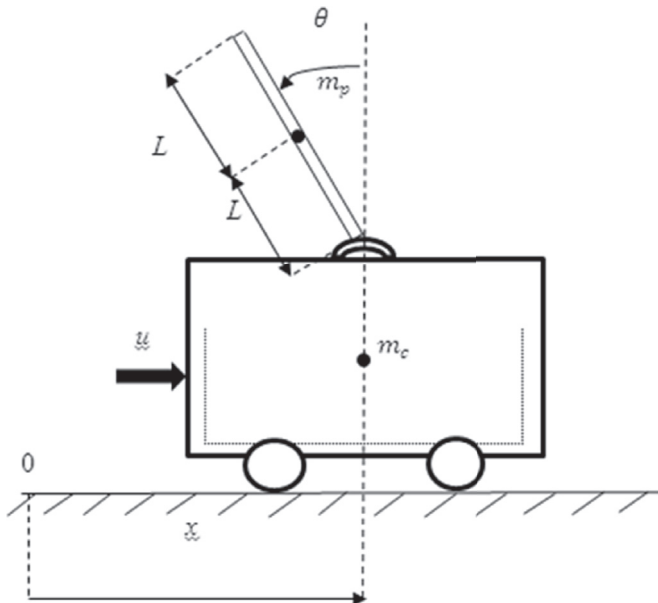


Fig. 1. Cart–pole system.

Table 1
Controller parameters of the cart–pole system.

Parameters	DSMC	DTSMC	ADTSMC	ASTDTSMC
λ_1	5	—	6	6
λ_2	0.5	—	0.6	0.7
K	10	64	10	—
ϕ_1	5	5	5	—
ϕ_2	—	—	5	—
ϕ_z	15	15	15	15
Z_U	0.9425	0.9425	0.9425	0.9425
q_1/p_1	—	19/21	19/21	19/21
q_2/p_2	—	17/21	17/21	17/21
L_1	—	—	—	50
L_2	—	—	—	1

vertical axis, $x_3(t)$ denotes the position of the cart, $x_4(t)$ indicates the cart velocity, m_t is the total mass of the system which contains the mass of the pole (m_p) and the mass of the cart (m_c), and L is the half-length of the pole. The disturbances and uncertainties terms are given as $d_1(t) = d_2(t) = 0.0873 \sin(t)$, $\Delta f_1(t) = 0.5 \sin(x_1(t))$ and $\Delta f_2(t) = 0.5 \sin(x_3(t))$. For the simulation purpose, the constant parameters and initial condition of the cart–pole system are considered as

$m_p = 0.05 \text{ kg}$, $m_c = 1 \text{ kg}$, $L = 0.5 \text{ m}$, $g = 9.8 \text{ m/s}^2$, $x(0) = [-60^\circ, 0, 0, 0]^T$. The parameters of the controllers are reported in Table 1.

In order to consider the stabilization problem, some performance indices are introduced in this section as follows:

(I) Integral of absolute value of error (IAE)

$$I_1 = \int_0^t |x_i(\tau)| d\tau \quad (30)$$

(II) Integral of time-multiplied absolute value of error (ITAE)

$$I_2 = \int_0^t \tau |x_i(\tau)| d\tau \quad (31)$$

The values of performance indices of cart–pole system for all of the methods are presented in Table 2. As it can be observed from Table 2, via the suggested control method, the performance indices for the states x_1 and x_3 are smaller in comparison with the results of the other methods. These results demonstrate the improved stabilization performance of the suggested technique over the other ones.

Time responses of the angular position of the pole are displayed in Fig. 2. It is concluded from Fig. 2 that the proposed ASTDTSMC scheme presents a faster and accurate response over the other methods. Fig. 3 demonstrates time trajectories of the position evolution of the cart. It is obtained from Fig. 3 that the suggested control method is able to maintain the cart in a shorter distance

Table 2
Computed IAE and ITAE values for the cart–pole system.

	IAE		ITAE	
	x_1	x_3	x_1	x_3
DSMC	35.9506	0.8578	42.5343	1.5366
DTSMC	17.6036	0.3110	8.6574	0.2132
ADTSMC	15.9849	0.3307	24.0808	0.7223
ASTDTSMC	15.6820	0.3001	6.6859	0.1182

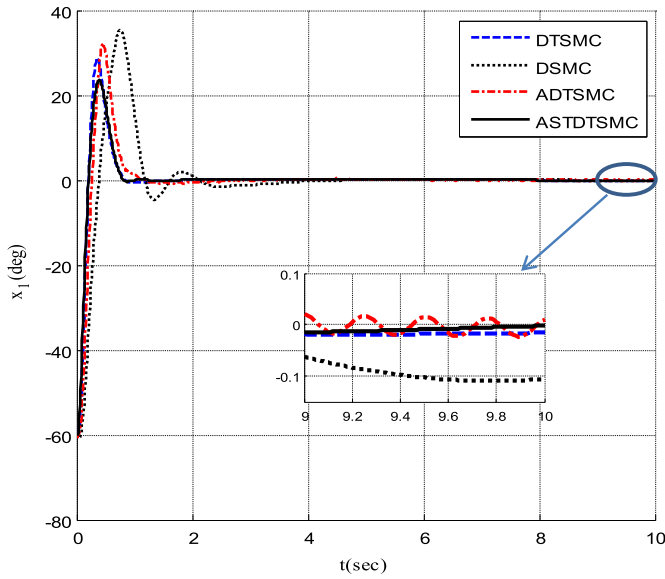


Fig. 2. Time histories of the angular position of the pole.

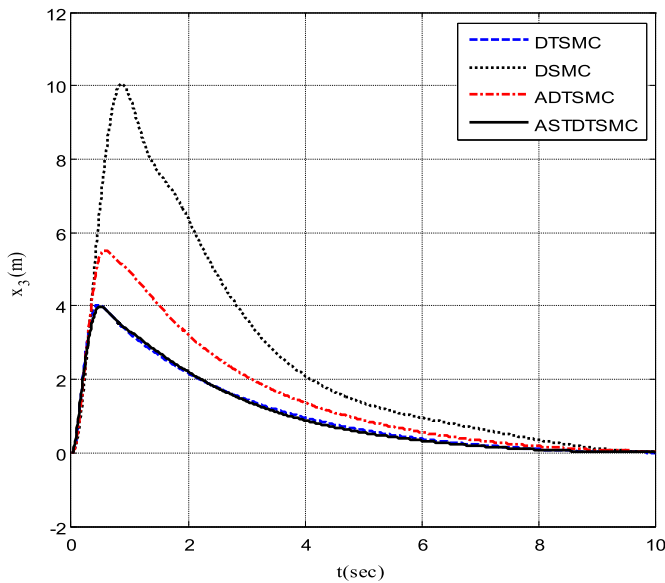


Fig. 3. Time trajectories of the position of the cart.

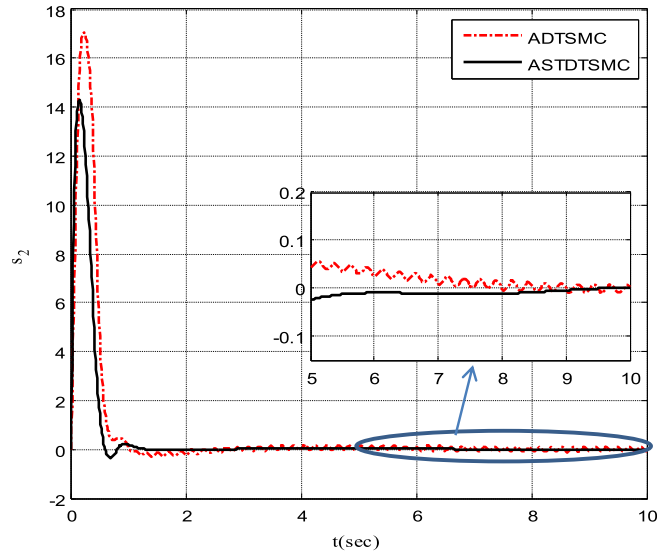
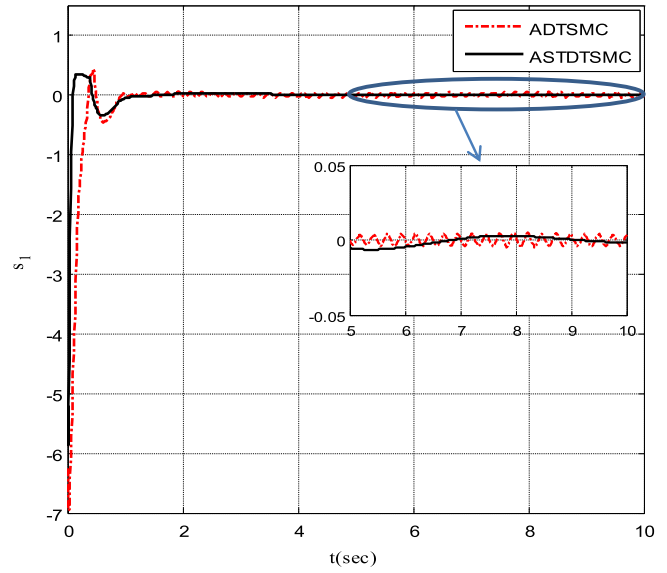


Fig. 4. Time responses of the sliding surfaces.

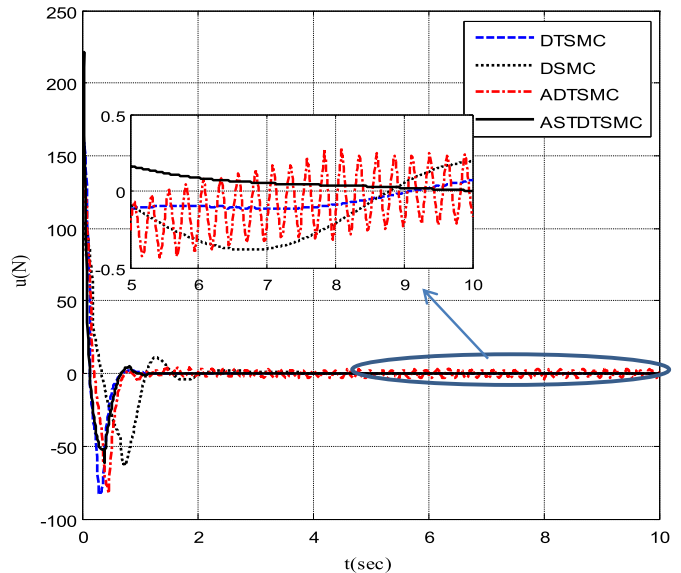


Fig. 5. Time histories of the control inputs.

which confirms that it is faster compared to the other techniques. Moreover, comparing the convergence speed of positions of the pendulum and cart, it is obviously observed from Figs. 2 and 3 that the cart has slower internal dynamics compared to that of the pendulum. Time histories of the sliding surfaces are shown in Fig. 4, which verifies that the proposed ASTDTSMC method has the chattering-free and smooth sliding surfaces in comparison with ADTSMC approach. The adaptation parameters are obtained as $\hat{\beta}_1 = 1.276$ (ADTSMC) and $\hat{\beta}_1 = 0.101$ (ASTDTSMC). Fig. 5 displays the time responses of the control inputs. It is obtained from Fig. 5 that the ADTSMC method suffers from the high-frequency oscillations, and the proposed ASTDTSMC scheme generates a faster control input.

In what follows, for the robustness analysis, the simulation studies are repeated with different values of the initial conditions, parametric uncertainties and external disturbances. The new

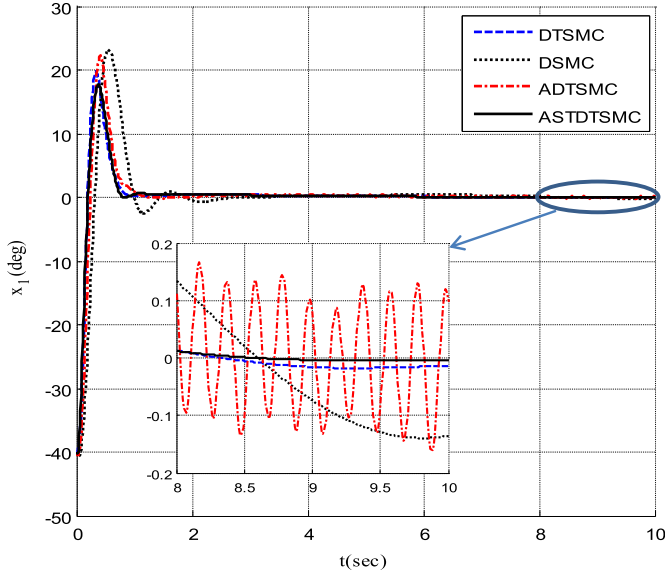


Fig. 6. Time responses of the pendulum angular position (with different conditions).

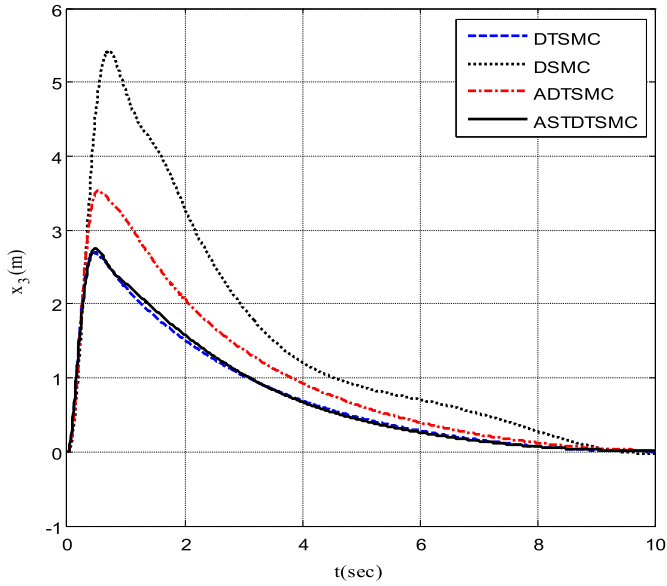


Fig. 7. Time histories of the cart position (with different conditions).

condition is specified as $x(0) = [-40^\circ, 0, 0, 0]^T$, $d_1(t) = d_2(t) = 0.1 \cos(t)$, $\Delta f_1(t) = 0.7 \sin(x_1(t))$ and $\Delta f_2(t) = 0.8 \sin(x_3(t))$. Time histories of the pendulum angular position, cart position, sliding surfaces and control signals are displayed in Figs. 6–9, respectively. These simulation results are similar to the previous studies, which confirm that the suggested control scheme has fine robust performance in different conditions, too.

Additionally, the experimental implementation of the suggested controller on the practical cart-pole system is executed via Matlab Real-Time and Simulink toolboxes. Fig. 10 shows the practical cart-pole system constructed in Department of Electrical Engineering in University of Zanjan. The pendulum angular position and cart linear position are measured by using E40S encoders of Autonics Company. The input-output data acquisition card is PCI-1751 which forms the connections between the computer and cart-pole system and contains the analog to digital and digital to analog converters.

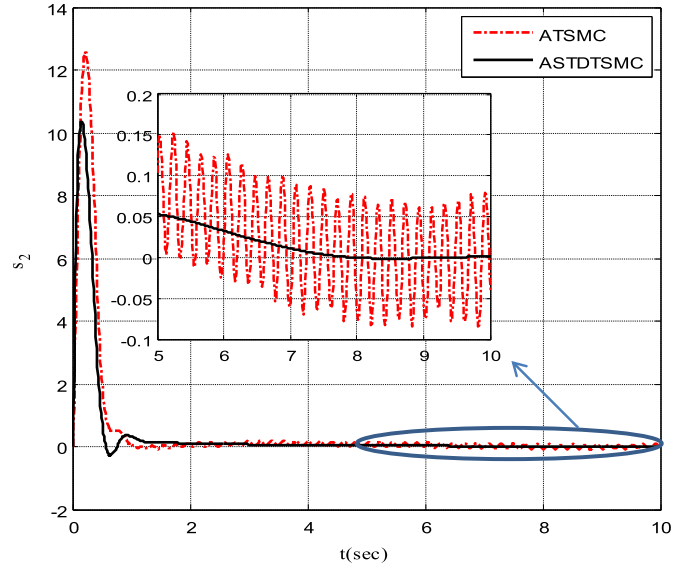
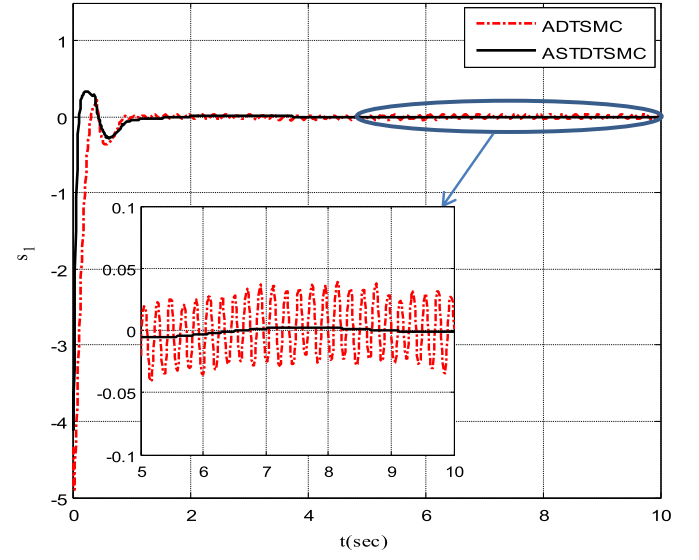
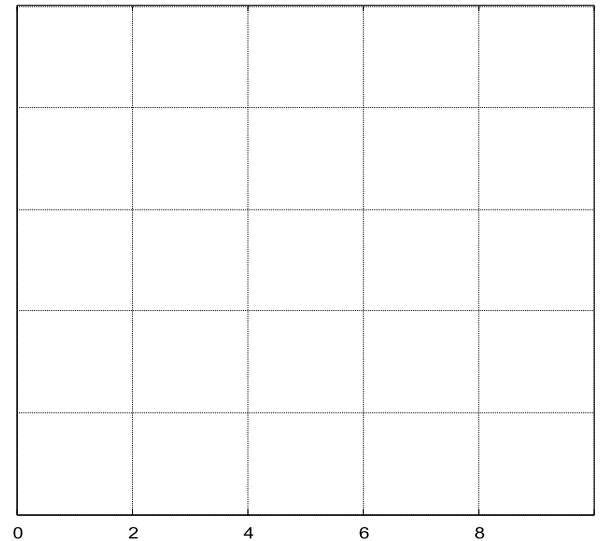


Fig. 8. Time trajectories of the sliding surfaces (with different conditions).



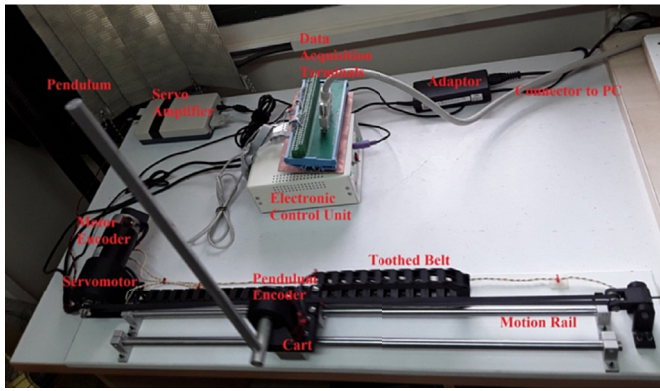


Fig. 10. The practical cart-pole system.

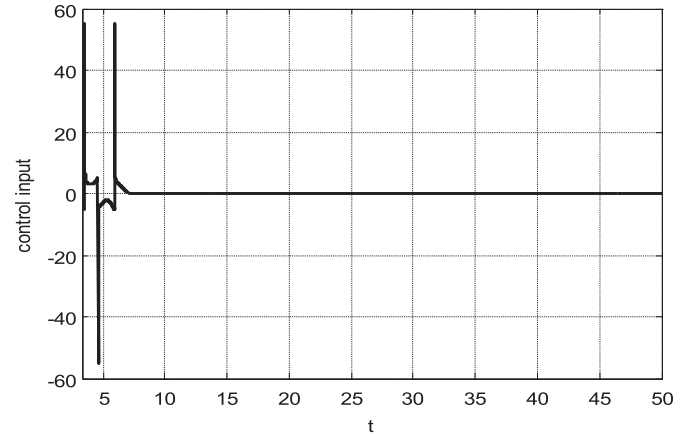


Fig. 13. Applied control signal.

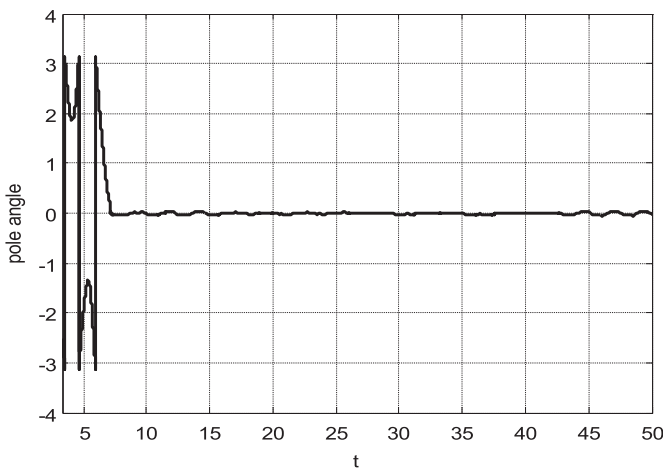


Fig. 11. Time history of angular position of the pole.

Experimental results for the angular position of the pole and linear position of the cart are presented in Fig. 11 and Fig. 12. It is easily shown that the angular position of the pole successfully varies from $-\pi$ rad to 0, and remains around zero afterward. The experimental results are consistent with numerical simulations which confirm the validity and effectiveness of the proposed scheme.

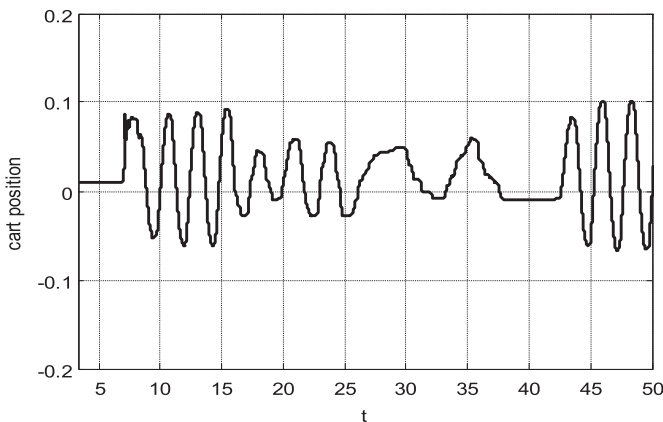


Fig. 12. Time response of linear position of the cart.

The applied control signal of the cart is illustrated in Fig. 13. It is shown that no chattering phenomenon is existed in the control input. In the experimental results, the swing-up time period has a high-amplitude control action. The experimental results confirm that the proposed control technique is successful in practice.

Remark 3. The chattering was excluded from our simulations for two reasons: the first reason is that in the proposed method, the time-derivative of w is applied in the suggested controller and the actual control signal achieved after integration procedure is continuous and chattering-free. The second reason is that the parameter L_2 is bigger than L_1 , which causes more influence of the term w in the control input (16).

5. Conclusions

In this article, a novel adaptive super-twisting decoupled terminal sliding mode control technique was suggested for a class of fourth-order systems. The planned scheme decoupled the nonlinear fourth-order systems into two second-order subsystems. The DTSMC technique was employed to force both subsystems converge to the equilibrium points in the finite time. The super-twisting algorithm eliminated the chattering phenomenon and the adaptive-tuning law avoided the requirement of the knowledge about the upper bounds of perturbations. The simulation results and experimental validations on the cart-pole system were presented to demonstrate the efficiency of the suggested technique over the other methods. Additionally, the recommended scheme demonstrates lower IAE and ITAE values compared with the existing control methods. As a future work, the adaptive-gain super-twisting global sliding mode control scheme can be employed to DTSMC approach to avoid the reaching phase and improve the robustness of the closed-loop system.

Declaration of conflicting interests

The authors declared no potential conflicts of interest with respect to the research, authorship, and/or publication of this article.

Acknowledgements

This research received no specific grant from any funding agency in the public, commercial, or not-for-profit sectors. The authors would like to thank Editor, Associate Editor and the anonymous reviewers for their much time and constructive comments to review and improve this paper.

References

- [1] Slotine J-JE, Li W. Applied nonlinear control. NJ: Prentice hall Englewood Cliffs; 1991.
- [2] Mobayen S, Baleanu D. Linear matrix inequalities design approach for robust stabilization of uncertain nonlinear systems with perturbation based on optimally-tuned global sliding mode control. *J Vib Contr* 2017;23: 1285–95.
- [3] Zheng E-H, Xiong J-J, Luo J-L. Second order sliding mode control for a quadrotor UAV. *ISA Trans* 2014;53:1350–6.
- [4] Khoo S, Xie L, Zhao S, Man Z. Multi-surface sliding control for fast finite-time leader–follower consensus with high order SISO uncertain nonlinear agents. *Int J Robust Nonlinear Control* 2014;24:2388–404.
- [5] Shtessel Y, Edwards C, Fridman L, Levant A. Sliding mode control and observation. Springer; 2014.
- [6] Ginoia D, Shendge P, Phadke S. Sliding mode control for mismatched uncertain systems using an extended disturbance observer. *IEEE Trans Ind Electron* 2014;61:1983–92.
- [7] Mondal S, Mahanta C. Chattering free adaptive multivariable sliding mode controller for systems with matched and mismatched uncertainty. *ISA Trans* 2013;52:335–41.
- [8] Yan J-J, Liao T-L. Discrete sliding mode control for hybrid synchronization of continuous Lorenz systems with matched/unmatched disturbances. *Trans Inst Meas Contr* 2017. <https://doi.org/10.1177/0142331216683773>.
- [9] González JA, Barreiro A, Dormido S, Baños A. Nonlinear adaptive sliding mode control with fast non-overshooting responses and chattering avoidance. *J Franklin Inst* 2017;354:2788–815.
- [10] Mobayen S. Finite-time stabilization of a class of chaotic systems with matched and unmatched uncertainties: an LMI approach. *Complexity* 2016;21:14–9.
- [11] Zhao D, Li S, Gao F. Finite time position synchronised control for parallel manipulators using fast terminal sliding mode. *Int J Syst Sci* 2009;40: 829–43.
- [12] Mobayen S, Baleanu D, Tchier F. Second-order fast terminal sliding mode control design based on LMI for a class of non-linear uncertain systems and its application to chaotic systems. *J Vib Contr* 2017;23:2912–25.
- [13] Mobayen S. Finite-time robust-tracking and model-following controller for uncertain dynamical systems. *J Vib Contr* 2016;22:1117–27.
- [14] Li J, Yang Y, Hua C, Guan X. Fixed-time backstepping control design for high-order strict-feedback non-linear systems via terminal sliding mode. *IET Control Theory & Appl* 2016;11:1184–93.
- [15] Mobayen S, Javadi S. Disturbance observer and finite-time tracker design of disturbed third-order nonholonomic systems using terminal sliding mode. *J Vib Contr* 2017;23:181–9.
- [16] Modirrousta A, Khodabandeh M. Adaptive non-singular terminal sliding mode controller: new design for full control of the quadrotor with external disturbances. *Trans Inst Meas Contr* 2017;39:371–83.
- [17] Al-Ghanimi A, Zheng J, Man Z. A fast non-singular terminal sliding mode control based on perturbation estimation for piezoelectric actuators systems. *Int J Contr* 2017;90:480–91.
- [18] Liu X, Han Y. Finite time control for MIMO nonlinear system based on higher-order sliding mode. *ISA Trans* 2014;53:1838–46.
- [19] Furat M, Eker I. Second-order integral sliding-mode control with experimental application. *ISA Trans* 2014;53:1661–9.
- [20] Xiong J-J, Zhang G-B. Global fast dynamic terminal sliding mode control for a quadrotor UAV. *ISA Trans* 2017;66:233–40.
- [21] Ma Z, Sun G. Dual terminal sliding mode control design for rigid robotic manipulator. *J Franklin Inst* 2017. <https://doi.org/10.1016/j.jfranklin.2017.01.034>.
- [22] Bayramoglu H, Komurcugil H. Nonsingular decoupled terminal sliding-mode control for a class of fourth-order nonlinear systems. *Commun Nonlinear Sci Numer Simulat* 2013;18:2527–39.
- [23] Bayramoglu H, Komurcugil H. Time-varying sliding-coefficient-based decoupled terminal sliding-mode control for a class of fourth-order systems. *ISA Trans* 2014;53:1044–53.
- [24] Bayramoglu H, Komurcugil H. Time-varying sliding-coefficient-based terminal sliding mode control methods for a class of fourth-order nonlinear systems. *Nonlinear Dynam* 2013;73:1645–57.
- [25] Mahmoodabadi MJ, Momennejad S, Bagheri A. Online optimal decoupled sliding mode control based on moving least squares and particle swarm optimization. *Inf Sci* 2014;268:342–56.
- [26] Xuemei N, Gao G, Liu X, Fang Z. Decoupled sliding mode control for a novel 3-DOF parallel manipulator with actuation redundancy. *Int J Adv Rob Syst* 2015;12:64.
- [27] Bejarano FJ, Fridman L. State exact reconstruction for switched linear systems via a super-twisting algorithm. *Int J Syst Sci* 2011;42:717–24.
- [28] Moreno JA, Osorio M. Strict Lyapunov functions for the super-twisting algorithm. *IEEE Trans Automat Contr* 2012;57:1035–40.
- [29] Salgado I, Chairez I, Camacho O, Yañez C. Super-twisting sliding mode differentiation for improving PD controllers performance of second order systems. *ISA Trans* 2014;53:1096–106.
- [30] Yang Y, Qin S, Jiang P. A modified super-twisting sliding mode control with inner feedback and adaptive gain schedule. *Int J Adapt Contr Signal Process* 2017;31:398–416.
- [31] Salgado I, Kamal S, Bandyopadhyay B, Chairez I, Fridman L. Control of discrete time systems based on recurrent super-twisting-like algorithm. *ISA Trans* 2016;64:47–55.
- [32] Levant A. Sliding order and sliding accuracy in sliding mode control. *Int J Contr* 1993;58:1247–63.
- [33] Zhang Y, Tang S, Guo J. Adaptive-gain fast super-twisting sliding mode fault tolerant control for a reusable launch vehicle in reentry phase. *ISA Trans* November 2017;71(2):380–90.
- [34] Zhang Y, Tang S, Guo J. Adaptive-gain fast super-twisting sliding mode fault tolerant control for a reusable launch vehicle in reentry phase. *ISA Trans* 2017;71:380–90.
- [35] Pati AK, Sahoo N. Adaptive super-twisting sliding mode control for a three-phase single-stage grid-connected differential boost inverter based photovoltaic system. *ISA Trans* 2017;69:296–306.
- [36] Kuntanapreeda S. Super-twisting sliding-mode traction control of vehicles with tractive force observer. *Contr Eng Pract* 2015;38:26–36.
- [37] Bejarano F, Fridman L, Poznyak A. Exact state estimation for linear systems with unknown inputs based on hierarchical super-twisting algorithm. *Int J Robust Nonlinear Control* 2007;17:1734–53.
- [38] Derafa L, Benallegue A, Fridman L. Super twisting control algorithm for the attitude tracking of a four rotors UAV. *J Franklin Inst* 2012;349:685–99.
- [39] Vaidyanathan S. Super-twisting sliding mode control and synchronization of moore-spiegel thermo-mechanical chaotic system. *Applications of Sliding Mode Control in Science and Engineering*. Springer; 2017. p. 451–70.
- [40] Salgado I, Chairez I, Bandyopadhyay B, Fridman L, Camacho O. Discrete-time non-linear state observer based on a super twisting-like algorithm. *IET Control Theory & Appl* 2014;8:803–12.
- [41] Levant A. Robust exact differentiation via sliding mode technique. *Automatica* 1998;34:379–84.
- [42] Bagheri A, Moghaddam JJ. Decoupled adaptive neuro-fuzzy (DANF) sliding mode control system for a Lorenz chaotic problem. *Expert Syst Appl* 2009;36: 6062–8.
- [43] Zhang Z, Xie Y, Le J, Chen L. Decoupled state-feedback and sliding-mode control for three-phase PWM rectifier. In: Power and energy engineering conference, 2009 APPEEC 2009 asia-pacific. IEEE; 2009. p. 1–5.
- [44] Mahmoodabadi M, Taherkhorsandi M, Talebipour M, Castillo-Villar K. Adaptive robust PID control subject to supervisory decoupled sliding mode control based upon genetic algorithm optimization. *Trans Inst Meas Contr* 2015;37:505–14.
- [45] Ivanescu M, Popescu D, Popescu N. A decoupled sliding mode control for a continuum arm. *Adv Robot* 2015;29:831–45.
- [46] Dhadekar DD, Patre B. UDE-based decoupled full-order sliding mode control for a class of uncertain nonlinear MIMO systems. *Nonlinear Dynam* 2017;88: 263–76.
- [47] Benhellal B, Hamerlain M, Rahmani Y. Decoupled adaptive neuro-interval Type-2 fuzzy sliding mode control applied in a 3DCrane system. *Arabian J Sci Eng* 2017;1–9.
- [48] Yang Y, Yan Y. Decoupled nonsingular terminal sliding mode control for affine nonlinear systems. *J Syst Eng Electron* 2016;27:192–200.
- [49] Zhao G, Li H, Song Z. Tensor product model transformation based decoupled terminal sliding mode control. *Int J Syst Sci* 2016;47:1791–803.
- [50] Wang W, Yi J, Zhao D, Liu D. Design of a stable sliding-mode controller for a class of second-order underactuated systems. *IEE Proc Contr Theor Appl* 2004;151:683–90.
- [51] Zhang X, Fang Y, Sun N. Minimum-time trajectory planning for underactuated overhead crane systems with state and control constraints. *IEEE Trans Ind Electron* 2014;61:6915–25.
- [52] Huang X, Yan Y, Huang Z. Finite-time control of underactuated spacecraft hovering. *Contr Eng Pract* 2017;68:46–62.
- [53] de Jesús Rubio J. Discrete time control based in neural networks for pendulums. *Appl Soft Comput* 2017. <https://doi.org/10.1016/j.asoc.2017.04.056>.
- [54] Aguilar-Ibanez C, Martínez-García JC, Soria-López A, Rubio JdJ. On the stabilization of the inverted-cart pendulum using the saturation function approach. *Math Probl Eng* 2011;2011:14.
- [55] Wang Z, Bao W, Li H. Second-order dynamic sliding-mode control for non-minimum phase underactuated hypersonic vehicles. *IEEE Trans Ind Electron* 2017;64:3105–12.
- [56] Mahjoub S, Mnif F, Derbel N. Second-order sliding mode approaches for the control of a class of underactuated systems. *Int J Autom Comput* 2015;12: 134–41.
- [57] Lo J-C, Kuo Y-H. Decoupled fuzzy sliding-mode control. *IEEE Trans Fuzzy Syst* 1998;6:426–35.